NASA Technical Memorandum 102175

Atomic Oxygen Degradation of Intelsat VI-Type Solar Array Interconnects: Laboratory Investigations

S. L. Koontz, J. B. Cross,
M. A. Hoffbauer, and
T. D. Kirkendahl

March 1991

NASA

NASA Technical Memorandum 102175

Atomic Oxygen Degradation of Intelsat VI-Type Solar Array Interconnects: Laboratory Investigations

S. L. Koontz
Lyndon B. Johnson Space Center
Houston, Texas

J. B. Cross and M. A. Hoffbauer
Los Alamos National Laboratory
Los Alamos, New Mexico

T. D. Kirkendahl
COMSAT Laboratories
Clarksburg, Maryland

National Aeronautics and Space Administration
Lyndon B. Johnson Space Center
Houston, Texas

March 1991

CONTENTS

TABLES

FIGURES

1.0 INTRODUCTION

The Intelsat VI communications satellite will be exposed to a number of space environment factors in low-Earth orbit that are absent or of limited importance in the geosynchronous mission profile originally planned for the vehicle. Evaluating the effect of low-Earth orbit environment factors on Intelsat VI vehicle materials and systems is the first step in deciding the fate of the satellite. The results of laboratory testing aimed at assessing the effects of low-Earth orbit atomic oxygen on the exposed silver interconnects in the Intelsat VI solar array are presented in this report. Laboratory testing became vital on finding that values of the reactivity of silver with atomic oxygen reported in the literature ranged over nearly two orders of magnitude and that the total number of published measurements is relatively small.

Tests were conducted on samples of silver interconnect material from the same production lot used to build the Intelsat VI solar arrays. In addition, configuration tests were conducted on a solar cell test article cut from a ground test solar array which is essentially identical to the Intelsat VI solar array. Atomic oxygen degradation of the interconnect silver was determined by: (1) mass loss after removing silver oxide, (2) scanning electron microscopy (SEM) thickness measurements after removal of silver oxide, (3) real-time electrical conductivity measurements (during oxygen atom exposure), (4) optical microscopy, (5) real-time solar cell performance (during oxygen atom exposure and thermal cycling).

The high velocity oxygen atom beam system at Los Alamos National Laboratory was used in the tests. The system was operated at a nominal atom kinetic energy of 2.0 eV, somewhat lower than the 5.0 eV expected on orbit. The system was operated at 2.0 eV instead of 5.0 because a turbopump failure limited vacuum system pumping speed. However, it should be noted that metallic silver, unlike many other materials, does not display a strong dependence of reactivity on oxygen atom translational energy. The test system was modified by incorporating a solar simulator lamp to generate operating photocurrents of ≈ 1 sun in the solar cell test article and, in addition, radiant heat for realistic thermal cycling.

Test specimens were exposed to total atom fluences comparable to the expected fluence for the Intelsat VI vehicle, on the order of 10^{21} atoms/square centimeter. The test specimens were held at various temperatures and, in some instances, subjected to thermal cycling during atom exposure to produce data describing the temperature dependence of the degradation reaction and the effects, if any, of thermal cycling.

2.0 O-ATOM PLASMA SOURCE AND EXPOSURE FACILITY

The O-atom source (figure 1) employs a continuous (not pulsed) plasma produced by focusing a high power CO_2 laser beam to produce plasma temperatures of 15,000-20,000 K in a rare-gas/oxygen mixture. The high power cw CO_2 laser (10.6 μm) is used to sustain a spark-initiated plasma in the mixture which subsequently flows through the throat (0.3 mm in diameter) of a hydrodynamic expansion nozzle producing an atomic beam of neutral species. Stagnation pressures of 2-8 atm are used depending on the rare gas, i.e., 2 atm for 50% O_2 in argon and 8 atm for 15% O_2 in helium. A 2.54-cm focal-length ZnSe lens is used to focus the laser beam to a 70-100 μm spot, producing power densities of 10^7 W/cm^2, thus sustaining the plasma at a roughly 50% ionized condition. The lens is moved axially to position the plasma ball in the throat of the water-cooled nozzle. Continuous operation times of greater than 75 hours have been obtained producing fluences $> 10^{22}$ O-atoms/cm^2. The source is mounted in a molecular beam apparatus (figure 2)

where the gas mixture is skimmed after exiting the nozzle and then collimated into a neutral atomic beam of rare gas and O-atoms. The facility consists of (1) the laser-sustained O-atom beam source, (2) three stages of differential pumping between the source and a sample manipulator located 15 cm from the source, (3) a rotatable mass spectrometer with time-of-flight (TOF) capability for measurements of scattered particle angular and velocity distributions to determine accommodation coefficients and gas phase reaction products, and (4) a flight instruments calibration chamber and a separate quadrupole mass spectrometer located 120 cm from the source which is used for beam TOF measurements. At the sample manipulator position, 15 cm from the source, O-atom flux densities of 5×10^{16} O-atoms/s-cm^2 are obtained, whereas at the flight mass spectrometer position, flux densities of 10^{15} O-atoms/s-cm^2 are recorded. A base pressure of 1×10^{-9} Torr is recorded in the sample exposure chamber, which rises to 2×10^{-6} Torr when the O-atom beam is operating. Figure 3 shows O-atom energy distributions obtained from TOF analysis of the beam. The rare-gas symbols indicate the oxygen/rare-gas composition; i.e., Ne designates a mixture of 50% Ne + 50% O_2, whereas Ne/He designates 25% O_2 + 25% Ne + 50% He. Also shown for comparison is the calculated in-orbit O-atom energy distribution assuming an atmospheric temperature of 1000 K. The percentage of dissociation for the mixtures Ar, Ne, Ne + He, and He are 85, 87, 96, and an estimated 98% at stagnation pressures of 1900, 2200, 4200, and 6000 Torr, respectively. The cw CO_2 laser power ranged from 1100 W for Ar/O_2 to 1600 W for He/O_2.

3.0 ATOMIC OXYGEN FLUX CALIBRATION

Absolute partial [C_i] number density measurements were made in the flight instruments chamber (figure 2) after thermal equilibration of the beam. An orifice of known diameter (1.270 cm) operating under effusive flow conditions was employed to pump on the chamber having a known temperature T. The composition of the high velocity beam was also measured using lock-in detection of the modulated beam and a residual gas analyzer corrected for known relative ionization cross sections. From these data, the partial flux density of each component of the high velocity beam was determined using a simple mass balance calculation on the inert gas component of the high velocity beam, i.e., the flux of inert gas entering the flight instruments chamber in the high velocity beam is equal to the flux of inert gas leaving the chamber by effusive flow through the orifice when the chamber pump is gated off. This technique produces O-atom flux values having a run-to-run variation of 20% and reaction efficiencies within 30% of the on-orbit measurements for polymeric materials.

4.0 RESULTS AND DISCUSSION

4.1 SOLAR CELL INTERCONNECTS

Typical SEM edge-on views of the Intelsat VI-type silver solar cell interconnects before exposure to the high velocity atomic oxygen beam are shown in figures 4 through 7. An average thickness of about 13 microns with a maximum thickness of about 20 microns is indicated, in agreement with dial caliper and metallographic measurements. Energy dispersive x-ray analysis of a silver interconnect specimen showed that the interconnect was 99% pure silver. X-ray photoelectron spectroscopy (XPS) of the surface showed silver to be the only metallic element with significant abundance. Sulfur and oxygen were the only other important elements to be detected by XPS, as would be expected for pure silver which had tarnished in air.

After a total fluence of 3×10^{20} oxygen atoms/square centimeter having a nominal atom energy of 2.0 eV, an interconnect specimen held at a temperature of 80 °C was visibly tarnished but showed no evidence of massive flaking of the oxide layer. Following dissolution of the silver oxide layer in aqueous ammonium hydroxide, SEM examination showed little or no change in interconnect thickness, as shown in figure 8. Metallographic analysis of the same specimen also showed little or no significant thickness change.

A second silver specimen was held at 75 °C for most of the atom fluence of 5.5×10^{20}. The 75 °C specimen was also subjected to two thermal cycles ranging from -40 to +50 °C. The interconnect specimen was weighed before exposure, after exposure, and after dissolution of the silver oxide formed. A mass loss of 0.121 mg was observed corresponding to a thickness loss of 4.6%, in reasonable agreement with the thickness measurements made on the 80 °C specimen. Figure 9 is a visible light photomicrograph showing the edge of the oxygen atom beam impingement area on the interconnect. The mass loss measurements reported above permit calculation of the stoichometry of the silver oxide film. An oxide film composition of $Ag_{1.78}$ O was obtained for the 75 °C oxide specimen.

Real-time measurements of the electrical conductance of the 80 °C silver interconnect specimen were made during the atomic oxygen exposure and the results are shown in figure 10. The small resistance change indicated is consistent with diffusion limited oxide growth kinetics as is shown by the good fit of a logarithmic relationship between oxygen atom fluence and conductance (figure 10). Similar results were obtained from the 75 °C sample as shown in figure 11. Differences in thermal history are the most likely explanation for the differences in the logarithmic laws obtained from the 75 and 80 °C data sets. It should be noted that no significant resistance changes could be measured with silver interconnect samples at 20 or 40 °C with comparable fluences of 2.0 eV oxygen atoms.

Thicker oxide layers and much larger resistance changes were obtained for silver interconnect samples at elevated temperatures, another result consistent with diffusion limited oxide growth. Edge-on SEM examination and metallographic analysis both showed an average thickness loss of about 30% for interconnect specimens exposed to a fluence of about 2×10^{20} oxygen atoms/square centimeter with interconnect temperatures of 125 and 150 °C. Once again, ammonium hydroxide was used to dissolve the silver oxide before SEM or metallography. An edge-on SEM view of the 150 °C, 2×10^{20} oxygen atom/square centimeter specimen (150 °C, a) after dissolution of the oxide layer is shown in figure 12. Comparison with figures 4 through 7 indicated that approximately 30% of the thickness of the silver interconnect has been lost. An optical photomicrograph of a second 150 °C (150 °C, b) specimen which received an oxygen atom fluence of 5.5×10^{20} is shown in figure 13. Comparison with figure 9 shows that higher temperatures result in a visibly thicker and rougher oxide film on the (150 °C, b) specimen than on the 80 °C specimen.

The (150 °C, b) specimen was weighed before and after exposure to the oxygen atom beam and after dissolution of the silver oxide layer. An oxide film stoichometry of $Ag_{1.85}$ O was obtained. 0.57 mg of silver was lost, corresponding to a 67% decrease in interconnect thickness.

Real-time electrical conductivity measurements on specimens (150 °C, a) and (150 °C, b) are shown in figures 14 and 15. At 150 °C, a logarithmic relationship between atom fluence and conductance similar to that reported above for the 80 °C samples (figures 10 and 11) is obtained when the atom fluence is less than 1.5×10^{20}. When atom fluence exceeds 1.5×10^{20}, the relationship between atom fluence and conductivity is approximately linear. The linear relationship obtained at higher oxygen atom fluences suggests a change in the mechanism of oxidation after a critical oxide film thickness is reached. The

change from a logarithmic to a linear law suggests that pores or cracks have developed in the oxide layer. Cracks or pores in the oxide layer give oxygen atoms more direct access to the underlying silver metal so that the rate limiting step in the oxidation is no longer transport of atoms, ions and electrons through a thick oxide film.

Thickness changes in the silver interconnect specimens were greater when measured by SEM or mass loss methods than when calculated from electrical conductance loss under all conditions investigated to date. This result suggests the formation of a conducting or semiconducting silver oxide layer on silver interconnect material which is exposed to a high velocity oxygen atom beam.

Additional thickness measurements on the test specimens described above were made by the Microelectronics Division of COMSAT Laboratories. The thickness of the various test articles was determined using a metallographic cross section technique after dissolving any surface oxide in ammonium hydroxide. The results are summarized in table I.

Table I. Thickness Measurements of INTELSAT VI Silver Interconnects After Atomic Oxygen Exposure by NASA/JSC at Los Alamos
(The silver oxide was dissolved by ammonium hydroxide at JSC)

Sample I.D.	At Ox Fluence atoms/cm^2	Ag Thickness Measured by JSC as Indicated	Ag Thickness Measured by COMSAT in Metallographic Cross Sections	
124 Silver (6/26/90)	Control (no exposure)	~13μm by SEM	14.0μm	
80 °C	3 × 10^{20} (2 eV)	No thickness change by SEM and metallographic cross section	11.9μm	
25 + 125 °C	~2 × 10^{20}	~30% loss by SEM	7.6μm	
150 °C (a)	~2 × 10^{20}	~30% loss by SEM	6.5μm	
Solar Cell Test Article	1 × 10^{20} (50 °C) + 2.5 × 10^{20} (30-130 °C)	3-10μm by SEM of severed loops	Intact loop Severed loop	7.6μm 6.5μm

Measurement of oxide formation kinetics at two different temperatures allows calculation of the activation energy for the oxidation process. An Arrhenius activation energy of 10-20 kcal/mole is indicated for the oxidation of Intelsat VI silver interconnect material, a result in good agreement with published values for the low temperature oxidation of silver.

4.2 SOLAR CELL TEST ARTICLE (STA)

A 5 × 5 cm segment (the Solar Cell Test Article or STA) was cut from a solar array test panel (Hughes Aircraft Company, Communications Satellite Division) used for engineering test during Intelsat VI development and identical in all important respects with the solar array on the Intelsat VI satellite. The STA was equipped with electrical leads to permit

real-time measurements of solar cell performance during atomic oxygen testing. In addition, a type K thermocouple was attached to the solar cell glass coverslip with an inorganic, non-outgassing, conductive epoxy to permit real-time temperature measurements of the cell during atomic oxygen testing. One of the two interconnect sets on the STA was cut prior to test so that the only current path between the two cells was the interconnect undergoing atomic oxygen bombardment. An optical photomicrograph of one of the STA interconnect loops before exposure to the atomic oxygen beam is shown in figure 16. The brushed metal surface is the top of the interconnect loop, and the translucent mass just below is silicone adhesive used to attach the glass coverslips to the solar cells. Apparently, the excess silicone adhesive was not removed from the assembly at the location of the interconnect loop. As a result, the side of each loop (and perhaps the top to a limited extent) is partly protected from atomic oxygen attack by a small mass of silicone adhesive.

The STA was exposed to the high velocity (2.0 eV) oxygen atom beam for 16 hours at a temperature of 50 °C and a fluence of 1×10^{20} oxygen atoms/square centimeter. During the first 16-hour exposure, cell resistance was measured and no attempt was made to produce photocurrent. Optical photomicrographs of each of the four interconnect loops after the 16-hour exposure are shown in figure 17. The development of some oxide tarnish and discoloration is evident. Considerable areas on three of the interconnect loops appear unaffected.

Next, a solar simulation lamp was installed in the high velocity atom beam system to permit simultaneous thermal cycling and generation of photocurrent for a better simulation of on-orbit conditions. The STA was then subjected to a fluence of 2.5×10^{20} oxygen atoms/square centimeter while being thermally cycled between about 30 and 130 °C. STA power output in Volt*amp units is plotted against atom fluence in figure 18. Cell temperature as measured with the front surface (coverslip) thermocouple is shown in figure 19. A total of 68 thermal/photo cycles were completed.

An optical photomicrograph of an STA interconnect loop immediately after completion of the thermal/photo cycles in the atomic oxygen beam is shown in figure 20. The oxide layer appears thicker and less of the virgin metal is visible.

The STA was then shipped to NASA Johnson Space Center (JSC) for further characterization. The mechanical shock and vibration of shipping appears to have loosened some of the oxide on the silver interconnect loops because a fine grey dust was found on the STA when the shipping container was opened. Optical photomicrographs taken at JSC (figure 21) show a rough, pitted surface on the interconnect loops, a result consistent with the removal of some oxide by mechanical shock and vibration.

The oxide on the STA interconnect loops was then dissolved in ammonium hydroxide. Optical photomicrographs of an interconnect loop before and after the oxide dissolution step are shown in figures 22 and 23. The surface of the interconnect loops becomes smoother and brighter on removal of the oxide but some surface roughness or pitting is still evident.

Two of the atomic oxygen damaged interconnect loops were then cut open for direct measurement of the thickness of the remaining silver by SEM. The STA was coated with about 500 angstroms of gold to prevent surface charging of insulating surfaces near the interconnects. The resulting scanning electron photomicrographs are shown in figures 24 and 25. The thickness of the remaining interconnect loop silver ranges from about 3 to 10 microns by this method. The STA was then shipped to the Microelectronics Division of COMSAT Laboratories for additional interconnect loop thickness measurements.

5.0 SUMMARY AND CONCLUSIONS

The degradation of Intelsat VI-type silver solar cell interconnects by high velocity oxygen atoms has been measured both for interconnect specimens and a segment of functioning solar array. The thickness of the oxide layer formed and its effect on the degradation kinetics depends strongly on the temperature of the silver interconnect. No spontaneous spalling or flaking of the silver oxide layer was observed at any temperature, though thick oxide layers, formed on the STA interconnects, did flake off to a limited extent during shipment from Los Alamos to JSC. Interconnect thickness loss was less than 5% for interconnect temperatures below 80 °C and oxygen atom fluences of up to 5.5×10^{20} atoms/square centimeter. Even lower thickness loss was calculated from changes in interconnect electrical conductance measured during oxygen atom exposure, suggesting that a conducting or semiconducting oxide forms on silver surfaces exposed to high velocity oxygen atoms. There were no detectable changes in interconnect electrical conductance with interconnect samples at 20 or 40 °C and comparable oxygen atom fluences.

Weight loss measurements allowed calculation of the stoichometry of the silver oxide films. The 75 °C interconnect specimen produced an $Ag_{1.78}$ O film, while the 150 °C specimen produced an $Ag_{1.85}$ O film. The oxides are oxygen rich compared to the expected Ag_2 O composition.

Both high and low temperature interconnect specimens showed logarithmic rates of conductance loss while in the oxygen atom beam over some range of atom fluences, a result consistent with slow diffusion of reactive species through a surface oxide barrier. An activation energy of 10-20 kcal/mole was calculated from the temperature dependence of oxide film growth kinetics in the logarithmic domain. A 150 °C specimen displayed a change from logarithmic to linear oxidation kinetics for oxygen atom fluences greater than 1.5×10^{20}. The change from logarithmic to linear oxidation kinetics indicates the development of cracks or pores in the surface oxide barrier layer. The 150 °C interconnect specimens showed a 30% thickness loss by SEM for a fluence of 2×10^{20} oxygen atoms (logarithmic kinetics) and a 67% decrease in silver thickness by mass loss for 5.5×10^{20} oxygen atoms (log kinetics to 1.5×10^{20} atoms/cm^2 then linear kinetics to 5.5×10^{20} atoms/cm^2).

The STA was exposed to 1×10^{20} oxygen atoms/square centimeter at a cell surface temperature of 50 °C and then to 2.5×10^{20} oxygen atoms/square centimeter while the STA was thermal/photo cycled between 30 and 130 °C 68 times. The same solar simulator lamp used to produce thermal cycling also produced photocurrent in the exposed cell interconnects, resulting in a more accurate reproduction of on-orbit conditions. Despite thermal cycling at much higher temperatures than are expected for the Intelsat VI itself, no degradation of cell output was observed after a total oxygen atom fluence of 3.5×10^{20} oxygen atoms/square centimeter. The remaining solar cell interconnect silver appears rough and pitted. Nonetheless, between 3 and 10 microns of silver remained as measured by SEM. Additional interconnect thickness measurements were made at COMSAT Laboratories and are reported in table 1.

The test results reported here imply that the silver interconnects on Intelsat VI will still have at least 80% of the starting thickness of silver metal by the time of the proposed satellite rescue mission in 1992.

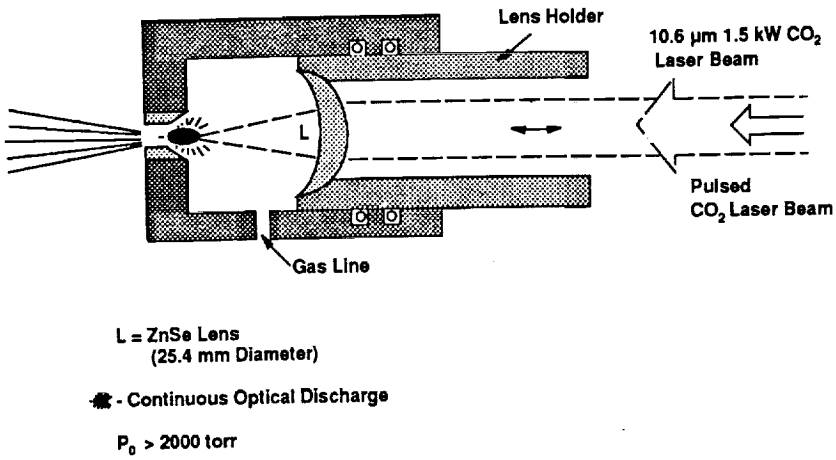

Figure 1.- Atomic Oxygen Nozzle: cw CO_2 laser sustains plasma which has a temperature between 12,000-15,000 K. O_2 rare-gas mixture is processed by the plasma/nozzle forming a high kinetic energy/intensity atomic beam.

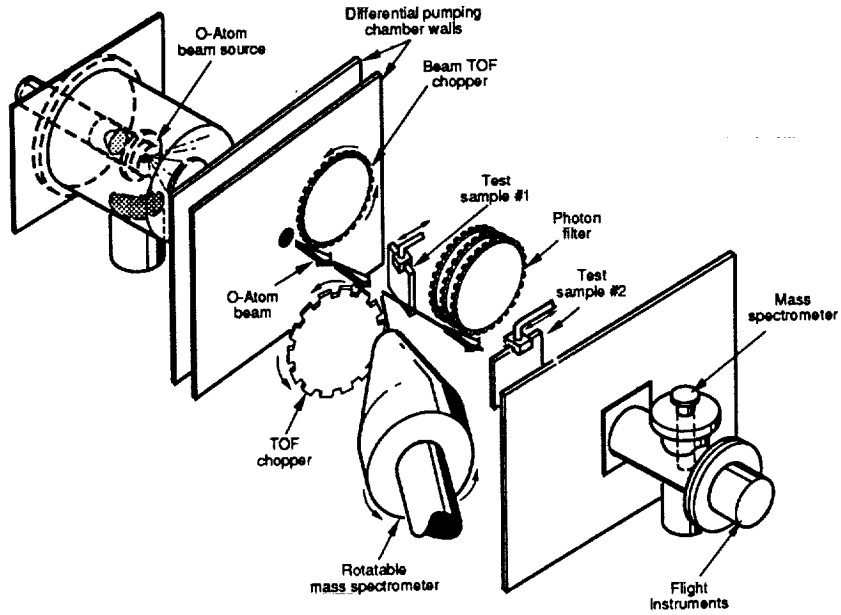

Figure 2.- Atomic Oxygen Exposure Facility: incorporates laser sustained plasma nozzle and mass spectrometric diagnostics.

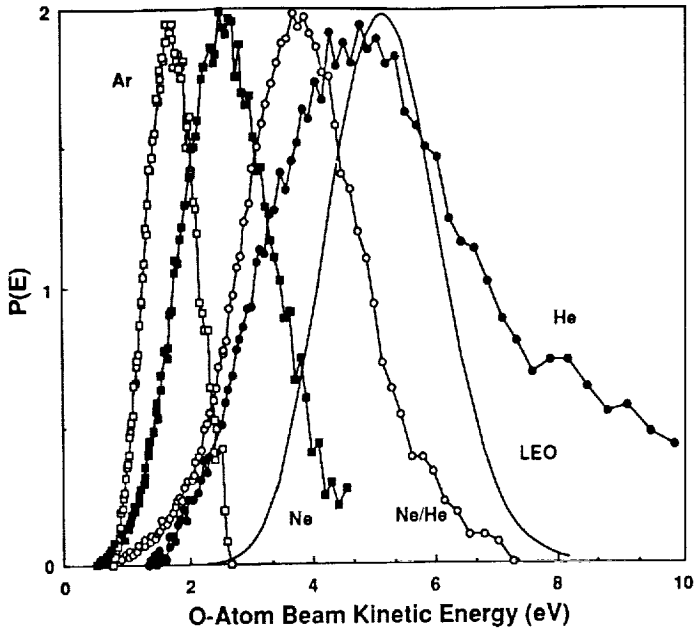

Figure 3.- Atomic Oxygen Kinetic Energy Distributions: rare gas symbols indicate a 50%-50% mixture of O_2/rare gas.

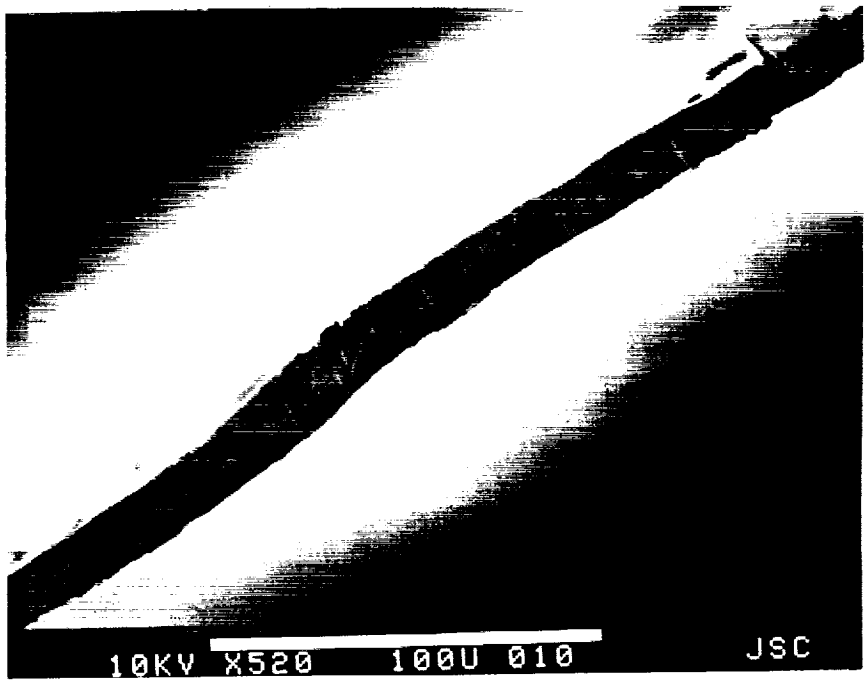

Figure 4.- SEM photograph of edge-on view of unexposed (reference picture) Intelsat VI interconnect silver foil. White bar at bottom of photograph represents 100 microns length. Enlargement factor of 520.

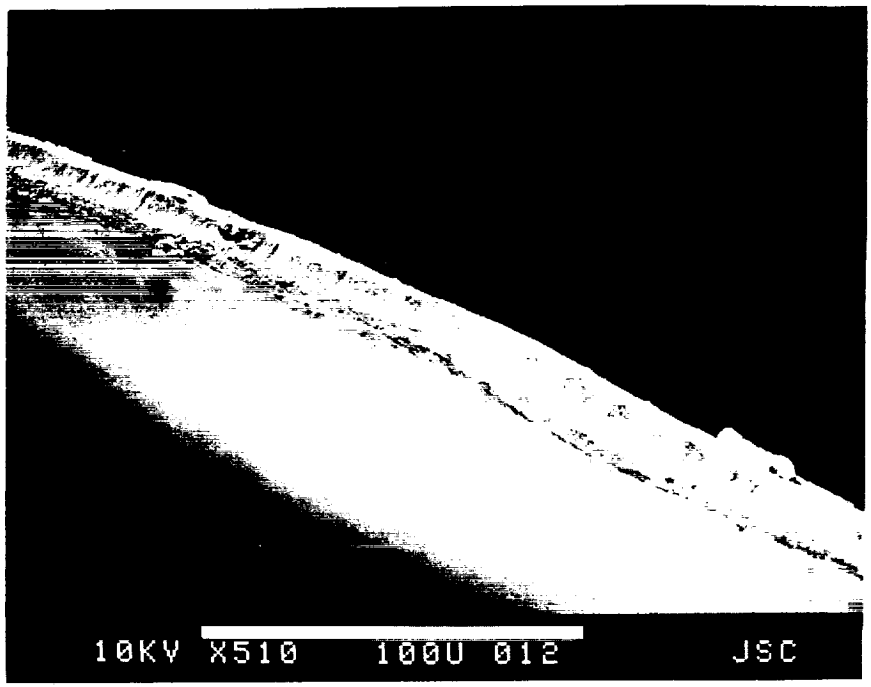

Figure 5.- SEM photograph of edge-on view of unexposed (reference picture) Intelsat VI interconnect silver foil. White bar at bottom of photograph represents 100 microns length. Enlargement factor of 510.

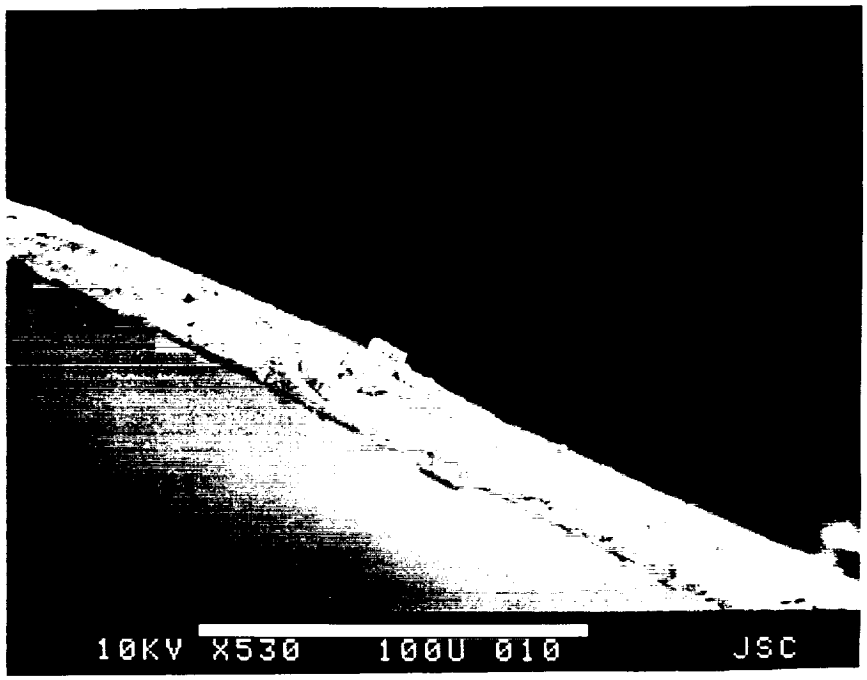

Figure 6.- SEM photograph of edge-on view of unexposed (reference picture) Intelsat VI interconnect silver foil. White bar at bottom of photograph represents 100 microns length. Enlargement factor of 530.

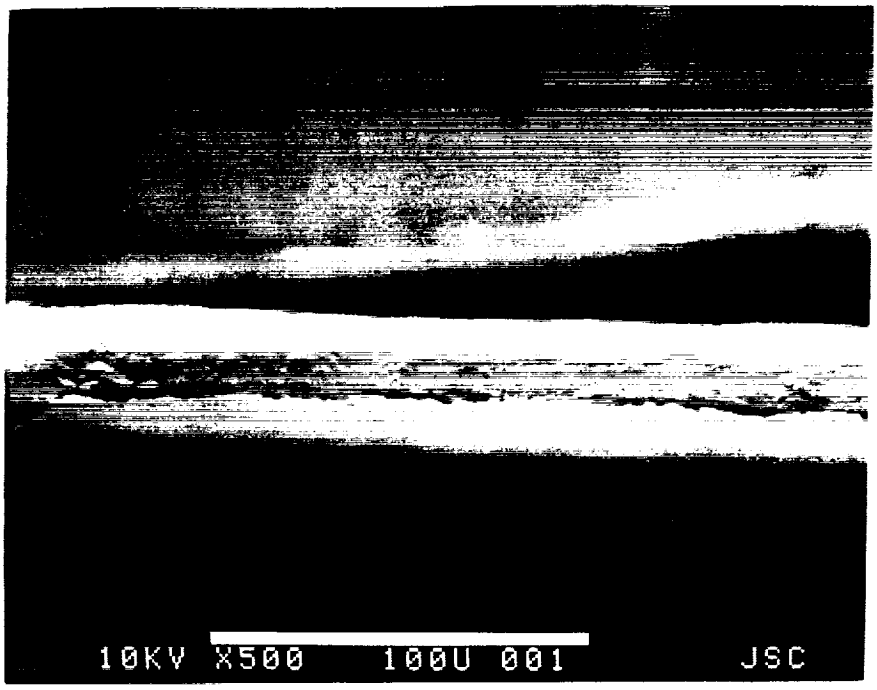

Figure 7.- SEM photograph of edge-on view of unexposed (reference picture) Intelsat VI interconnect silver foil. White bar at bottom of photograph represents 100 microns length. Enlargement factor of 500.

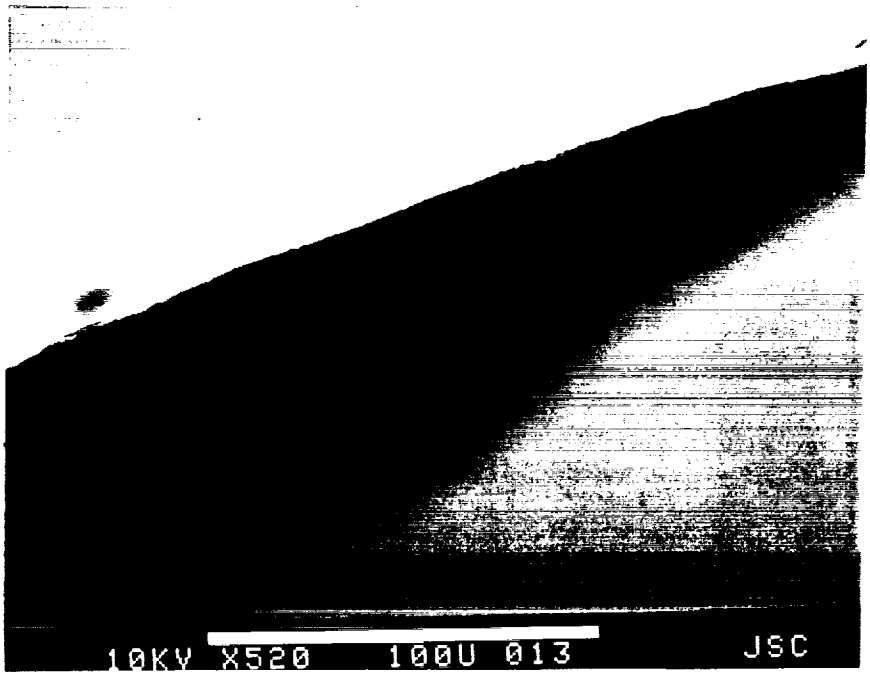

Figure 8.- SEM photograph of edge-on view of exposed (T = 80 °C) Intelsat VI interconnect silver foil. White bar at bottom of photograph represents 100 microns length. Enlargement factor of 520.

ORIGINAL PAGE
BLACK AND WHITE PHOTOGRAPH

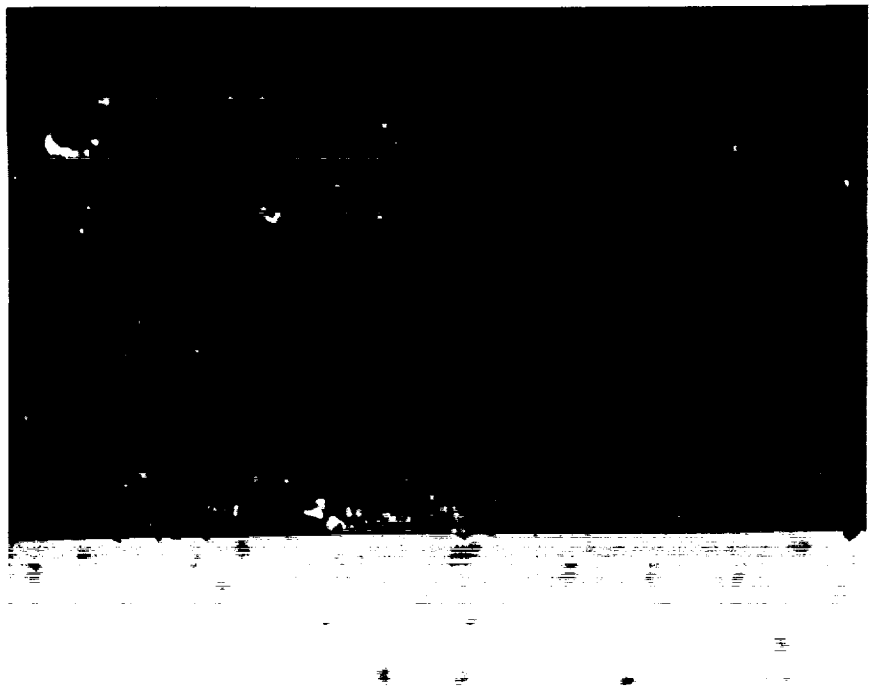

Figure 9.- Visible light photomicrograph of exposed (T = 75 °C) Intelsat VI interconnect silver foil. Enlargement factor of 115.

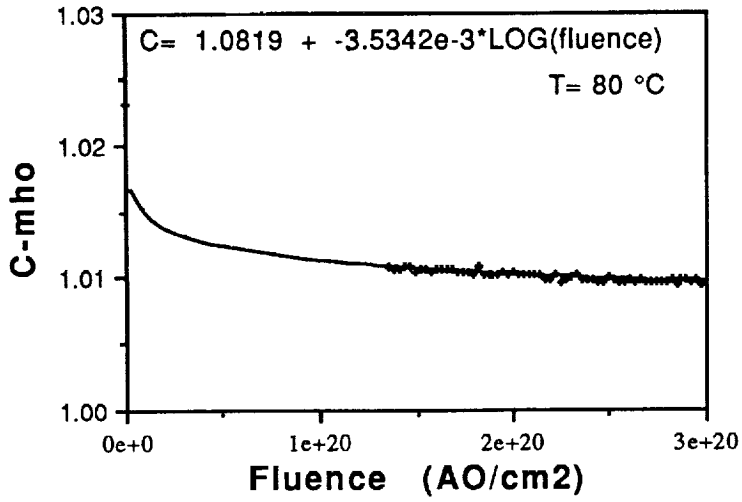

Figure 10.- Electrical conductance of silver interconnect at 80 °C as a function of atomic oxygen fluence. Note logarithmic fit to data.

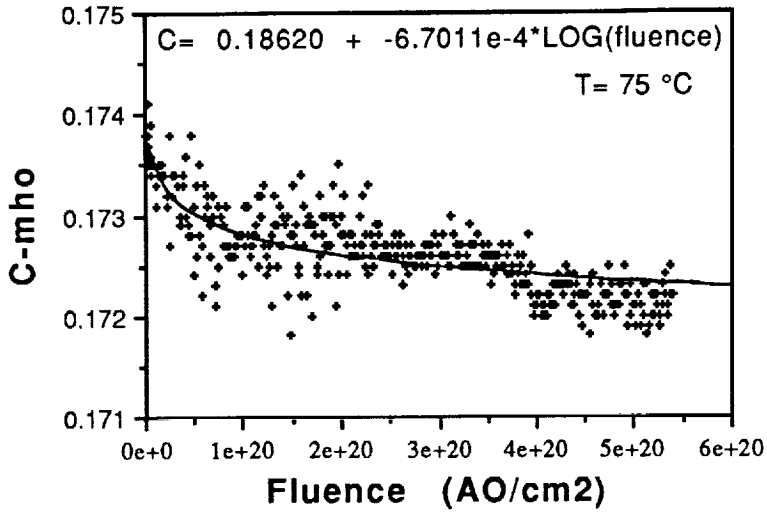

Figure 11.- Electrical conductance of silver interconnect at 75 °C as a function of atomic oxygen fluence. Note logarithmic fit to data.

ORIGINAL PAGE
BLACK AND WHITE PHOTOGRAPH

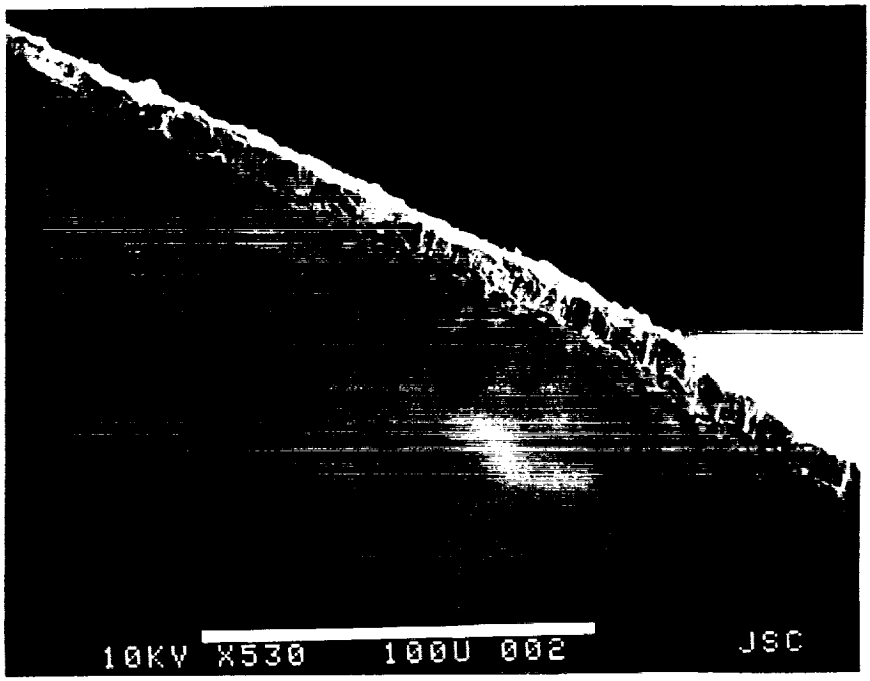

Figure 12.- SEM photograph of edge-on view of exposed (T = 150 °C) Intelsat VI interconnect silver foil. White bar at bottom of photograph represents 100 microns length. Enlargement factor of 530.

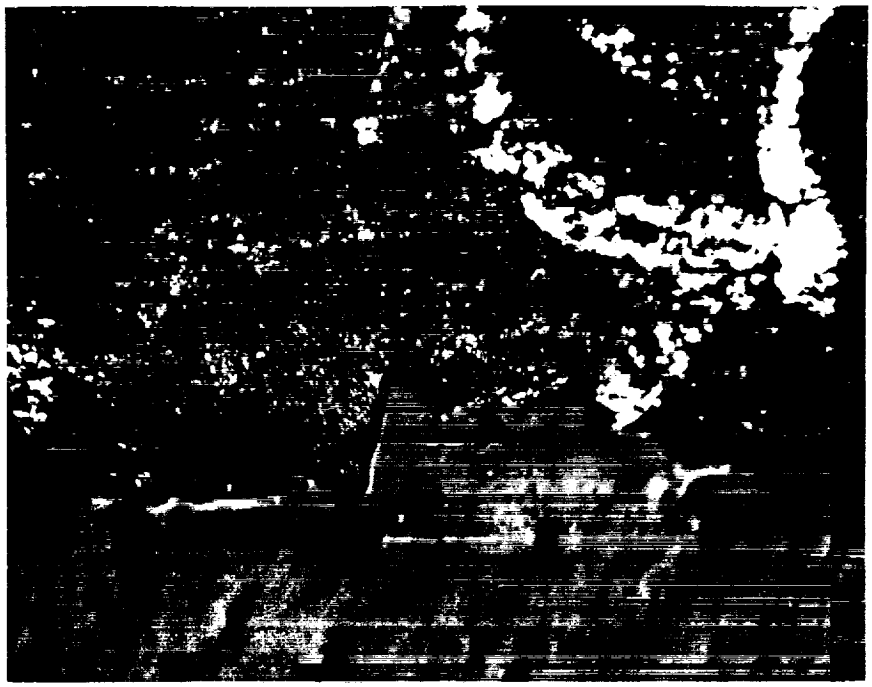

Figure 13.- Optical photomicrograph of Intelsat VI silver interconnect after exposure at 150 °C to atomic oxygen. Enlargement factor of 115.

ORIGINAL PAGE
BLACK AND WHITE PHOTOGRAPH

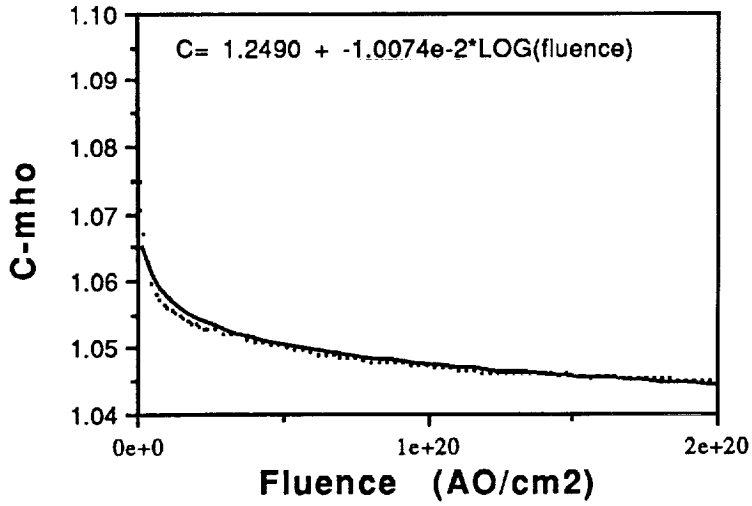

Figure 14.- Electrical conductivity of Intelsat VI silver interconnect foil at T < 150 °C,a. Note logarithmic relationship between conductance and O-atom fluence.

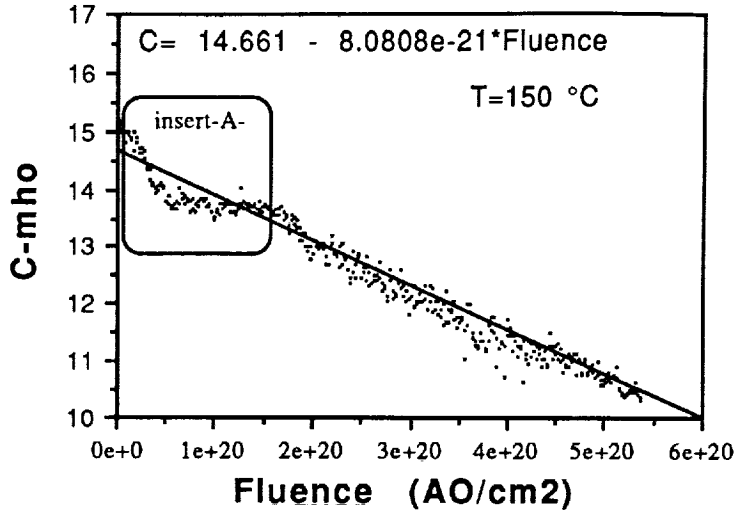

Figure 15.- Electrical conductivity of Intelsat VI silver interconnect foil at T > 150 °C,b. Note logarithmic relationship between conductance and O-atom fluence in insert -A- and then change over to a linear relationship.

ORIGINAL PAGE
BLACK AND WHITE PHOTOGRAPH

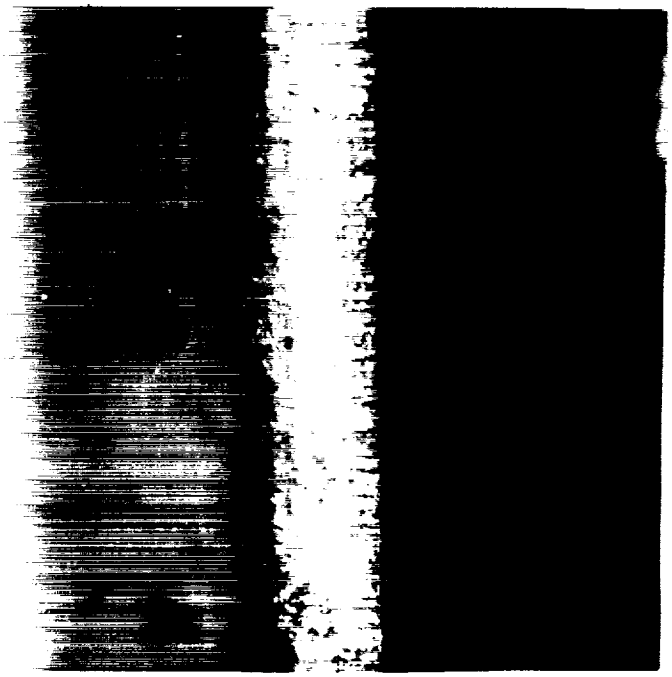

Figure 16.- Optical photomicrograph of the solar cell test article interconnect before exposure to atomic oxygen. Enlargement factor of 115.

ORIGINAL PAGE
BLACK AND WHITE PHOTOGRAPH

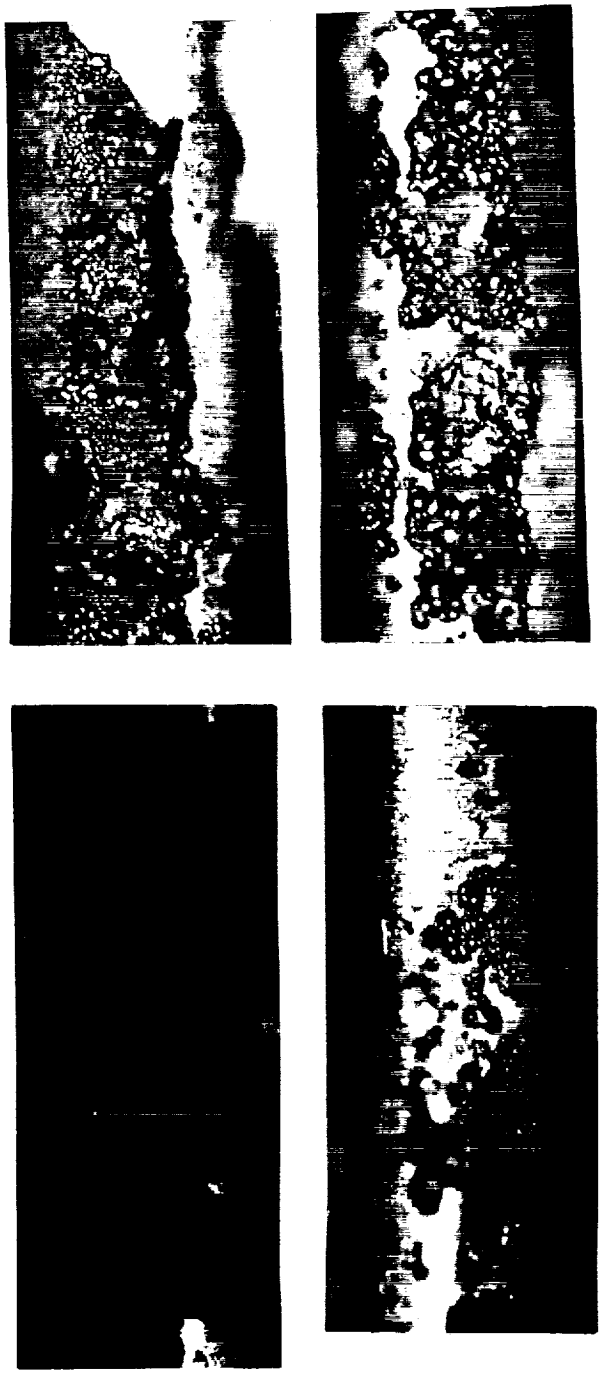

Figure 17.- Optical photomicrographs of four interconnect loops on solar cell test article after 16 hours of atomic oxygen exposure.

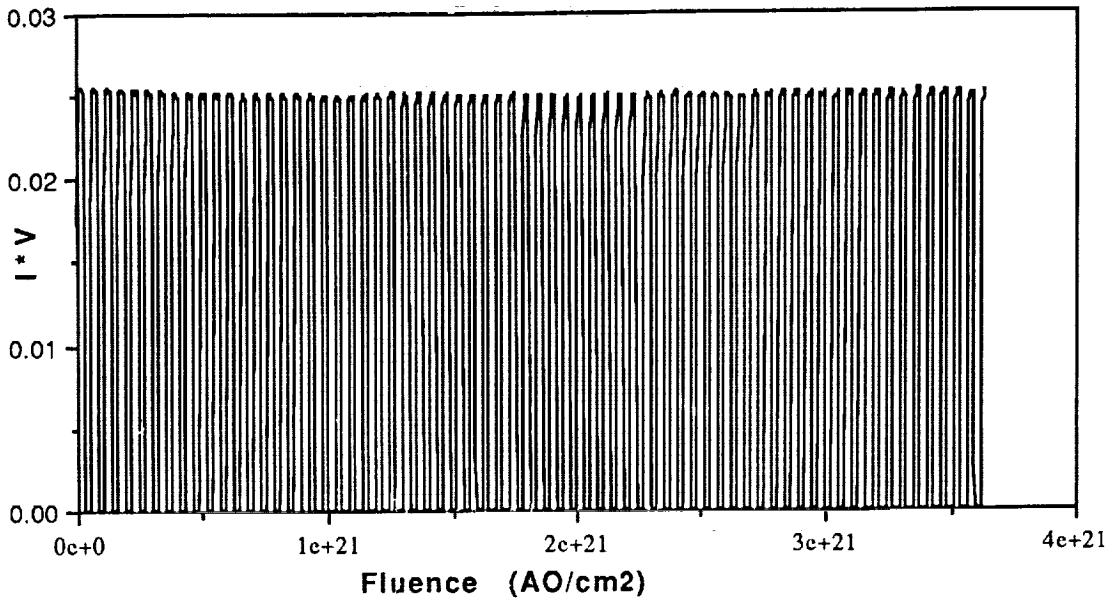

Figure 18.- Solar cell test article power output during thermal cycling and atomic oxygen exposure.

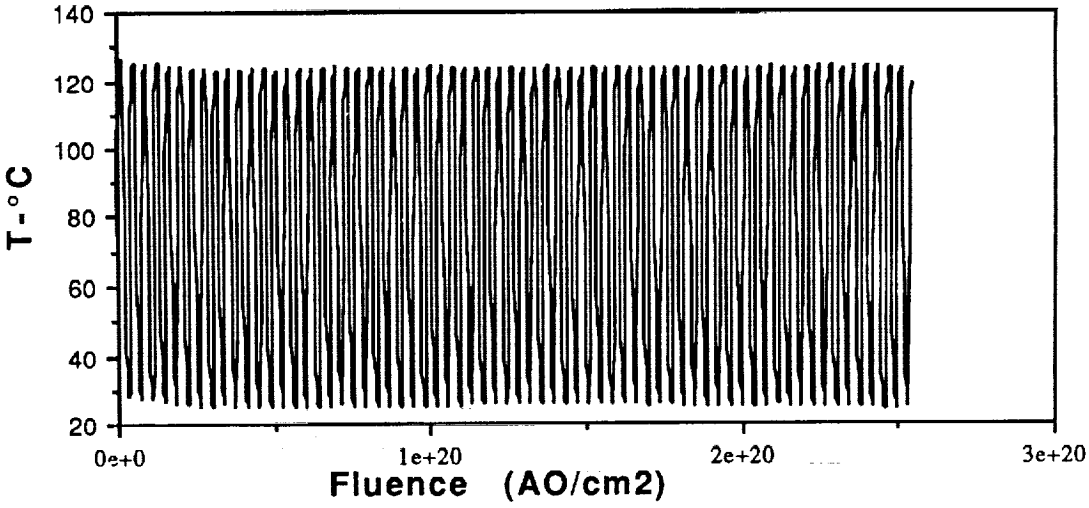

Figure 19.- Temperature variation of solar cell test article during thermal cycling and atomic oxygen exposure.

Figure 20.- Optical photomicrograph of solar cell test article immediately after completion of thermal cycling and atomic oxygen exposure.

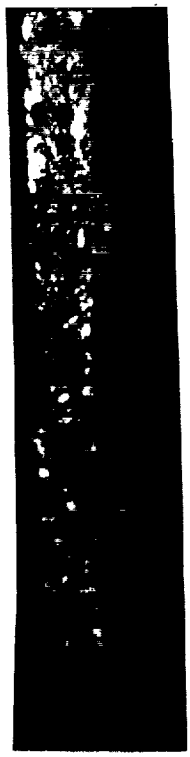

Figure 21.- Optical photomicrograph taken after mechanical shock and vibration during shipping.

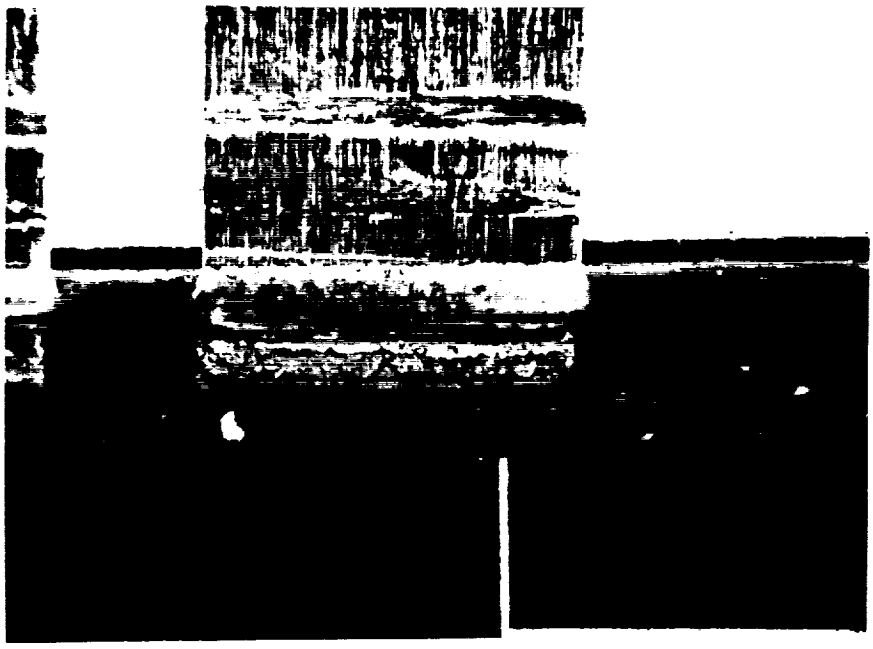

Figure 22.- Optical photomicrograph of solar cell interconnect loop before ammonium hydroxide treatment.

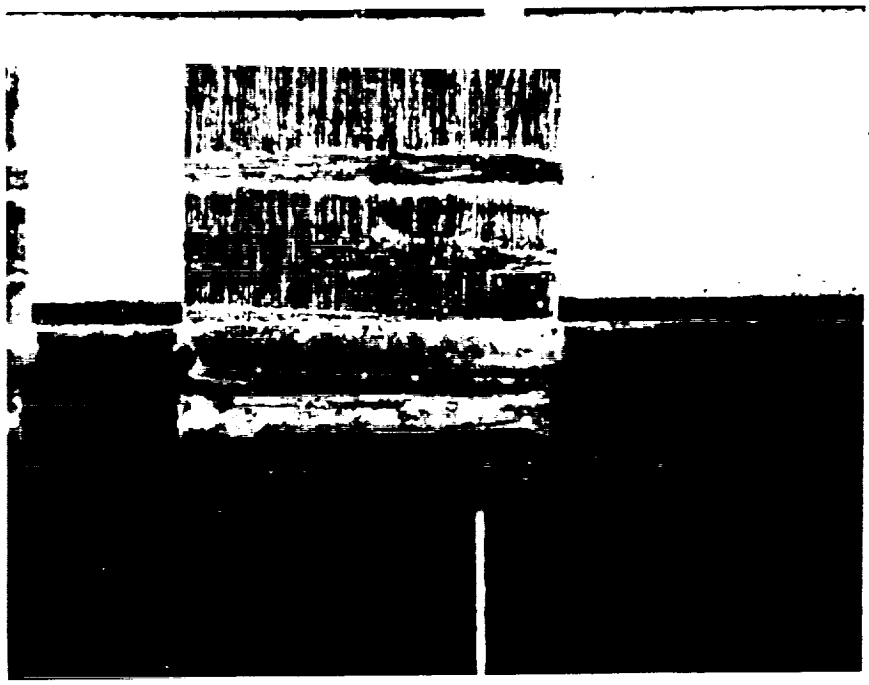

Figure 23.- Optical photomicrograph of photocell interconnect loop after oxide dissolution by ammonium hydroxide.

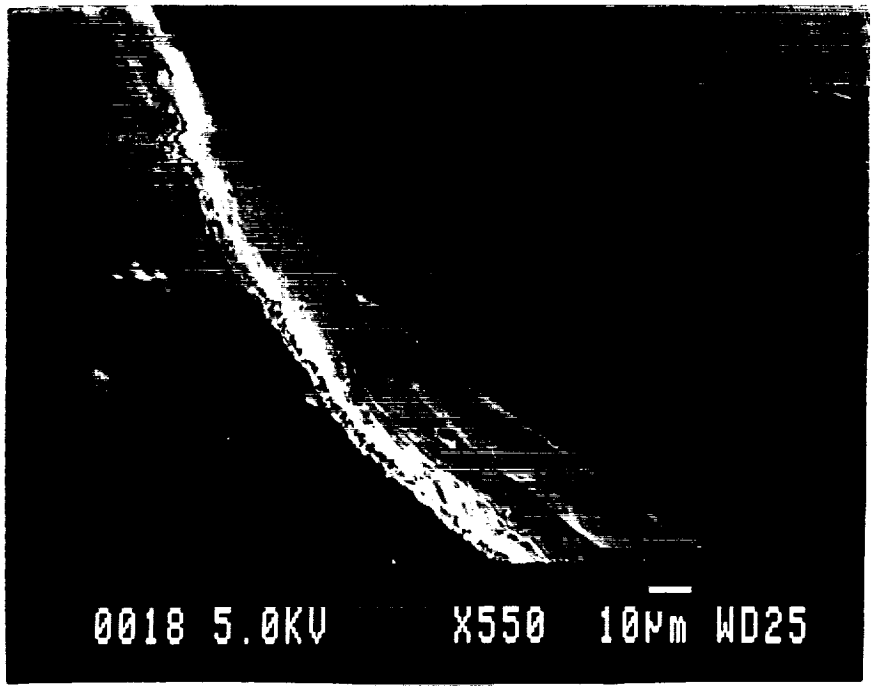

Figure 24.- SEM photograph of solar cell interconnect loop after thermal cycling, atomic oxygen exposure, and NH_4OH treatment.

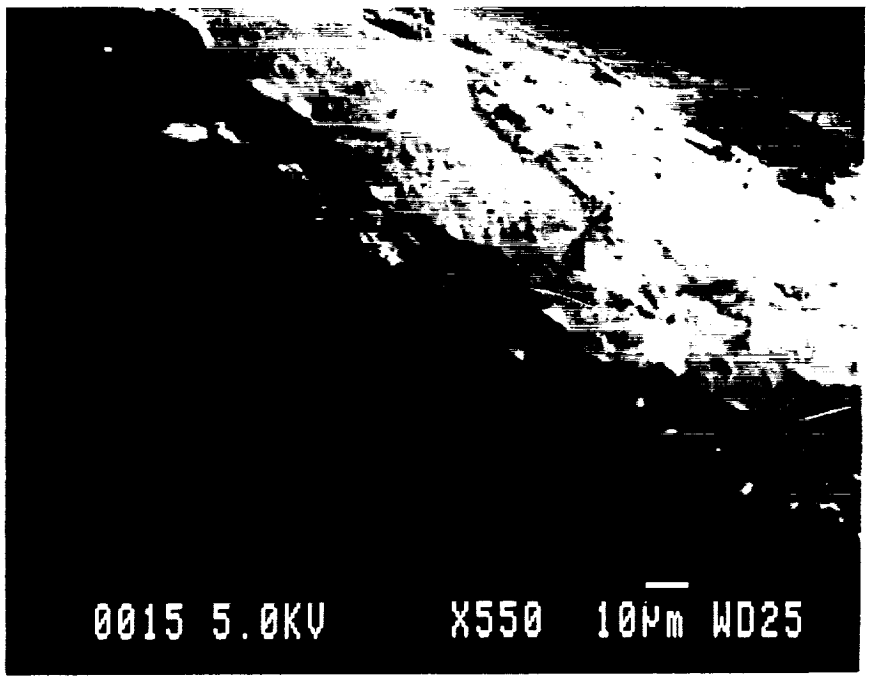

Figure 25.- SEM photograph of solar cell interconnect loop after thermal cycling, atomic oxygen exposure, and NH_4OH treatment.

NASA
National Aeronautics and Space Administration

REPORT DOCUMENTATION PAGE

1. Report No.	2. Government Accession No.	3. Recipient's Catalog No.
TM 102175		

4. Title and Subtitle	5. Report Date
Atomic Oxygen Degradation of Intelsat VI-Type Solar Array Interconnects: Laboratory Investigations	March 1991
	6. Performing Organization Code: ES 531
7. Author(s): S.L. Koontz (JSC), J.B. Cross and M.A. Hoffbauer (Los Alamos National Laboratory), and T.D. Kirkendahl (COMSAT Laboratories)	8. Performing Organization Report No.: S-625
9. Performing Organization Name and Address: Structures and Mechanics Division, National Aeronautics and Space Administration, Johnson Space Center	10. Work Unit No.
	11. Contract or Grant No.
12. Sponsoring Agency Name and Address	13. Type of Report and Period Covered: Technical Memorandum
	14. Sponsoring Agency Code

15. Supplementary Notes
Describes ground-based testing results in support of Intelsat VI Satellite rescue mission.

16. Abstract
A Hughes 506-type communications satellite belonging to the Intelsat organization was marooned in low-Earth orbit on March 14, 1990, following failure of the Titan third stage to separate properly. The satellite, Intelsat VI, was designed for service in geosynchronous orbit and contains several material configurations which are susceptible to attack by atomic oxygen. Analysis showed the silver foil interconnects in the satellite photovoltaic array to be the key materials issue because the silver is exposed directly to the atomic oxygen ram flux. This Technical Memorandum reports the results of atomic oxygen degradation testing of Intelsat VI-type silver foil interconnects both as virgin material and in a configured solar cell element. Test results indicate that more than 80 percent of the original thickness of silver in the Intelsat VI solar array interconnects should remain after completion of the proposed Space Shuttle rescue/reboost mission.

17. Key Words (Suggested by Author(s))
atomic oxygen, materials degradation, silver, solar cell, solar photovoltaic, high-velocity O atom beam, low-Earth orbit

18. Distribution Statement
Unlimited Distribution
Subject Category 26

19. Security Classification (of this report)	20. Security Classification (of this page)	21. No. of pages	22. Price
Unclassified	Unclassified		

For sale by the National Technical Information Service, Springfield, VA 22161-2171